




Cite this: *Green Chem.*, 2017, **19**, 3032

## A solid acetylene reagent with enhanced reactivity: fluoride-mediated functionalization of alcohols and phenols†

Georg Werner,<sup>a</sup> Konstantin S. Rodygin,<sup>a</sup> Anton A. Kostin,<sup>a</sup> Evgeniy G. Gordeev,<sup>b</sup> Alexey S. Kashin<sup>b</sup> and Valentine P. Ananikov  <sup>\*a,b</sup>

The direct vinylation of an OH group in alcohols and phenols was carried out utilizing a novel  $\text{CaC}_2/\text{KF}$  solid acetylene reagent in a simple  $\text{K}_2\text{CO}_3/\text{KOH}/\text{DMSO}$  system. The functionalization of a series of hydroxyl-group-containing substrates and the post-modification of biologically active molecules were successfully performed using standard laboratory equipment, providing straightforward access to the corresponding vinyl ethers. The overall process developed involves an atom-economical addition reaction employing only inorganic reagents, which significantly simplifies the reaction set-up and the isolation of products. A mechanistic study revealed a dual role of the  $\text{F}^-$  additive, which both mediates the surface etching/renewal of the calcium carbide particles and activates the  $\text{C}\equiv\text{C}$  bond towards the addition reaction. The development of the fluoride-mediated nucleophilic addition of alcohols eliminates the need for strong bases and may substantially extend the areas of application of this attractive synthetic methodology due to increasing functional group tolerance. As a replacement for dangerous and difficult to handle high-pressure acetylene, we propose the solid reagent  $\text{CaC}_2/\text{KF}$ , which is easy to handle, does not require dedicated laboratory equipment and demonstrates enhanced reactivity of the acetylenic triple bond. Theoretical calculations have shown that fluoride-mediated activation of the hydroxyl group towards nucleophilic addition significantly reduces the activation barrier and facilitates the reaction.

Received 9th March 2017,  
Accepted 2nd May 2017

DOI: 10.1039/c7gc00724h

rsc.li/greenchem

## Introduction

The post-modification of complex molecules is becoming an urgent topic due to the high-cost and time-consuming total syntheses of pharmaceutical substances, biologically active compounds and smart material building blocks.<sup>1</sup> Indeed, in the case of a multistep synthesis (Fig. 1A), the incorporation of a new functionality into complex molecules would require the repetition of the whole procedure using a modified starting reagent (Fig. 1B). Late-stage functionalization is an alternative approach, which gives access to the desired product from the available molecule in a single step, avoiding *de novo* preparation (Fig. 1C). This flexible concept opens up new possibilities to a range of modified complex molecules.

The hydroxyl functional group represents one of the most essential building blocks for a diverse range of biologically

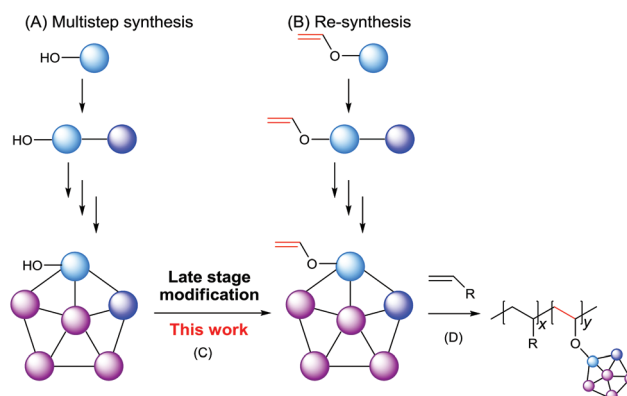


Fig. 1 Preparation of vinyl derivatives: common multistep synthesis vs. late-stage modification.

<sup>a</sup>Saint Petersburg State University, Universitetskyy pr. 26, Stary Petergof 198504, Russia

<sup>b</sup>Zelinsky Institute of Organic Chemistry, Russian Academy of Sciences, Leninsky pr. 47, Moscow 119991, Russia. E-mail: val@ioc.ac.ru; http://AnanikovLab.ru

†Electronic supplementary information (ESI) available. CCDC 1444527 and 1444530. For ESI and crystallographic data in CIF or other electronic format see DOI: 10.1039/c7gc00724h

and pharmacologically active substances. Consequently, the late-stage functionalization of an OH group is of great importance for turning on/off a direct interaction with an OH group and for adjusting the hydrophilic/hydrophobic properties of molecules (Fig. 1C). In addition, the facile preparation of well-defined and multifunctional polymers is of paramount signifi-



cance for the development of polymer-based drug carriers (Fig. 1D). This type of a polymer with enhanced biocompatibility, biodegradability and structural versatility contains attractive potential candidates for theranostic applications.<sup>2</sup>

Since vinyl ethers are common cationically polymerizable monomers and can undergo living polymerization to form well-defined polymers with desired molecular weights, modified drugs bearing *O*-vinyl groups can serve as suitable building blocks to attain this goal.<sup>3</sup>

The reaction of alcohols and phenols with gaseous acetylene is a direct route for the generation of *O*-vinyl ethers. This could be a promising practical methodology, which utilizes atom-economical transformations of alkynes in synthetic conversions.<sup>4–7</sup> However, the need for harsh reaction conditions, expensive equipment and special safety requirements for handling acetylene under high pressure make this approach difficult for application in research laboratories.<sup>8</sup> The use of strong bases and high temperature to activate alcohols towards nucleophilic addition<sup>6</sup> imposes drastic limitations on the reaction scope and reduces functional group tolerance (Fig. 2). Another drawback of the existing base-mediated reactions originates from a side-reaction of rapid oligomerization of the vinyl ethers during the synthesis, resulting in a significant drop in the product yield. Gaseous and *in situ* generated acetylene have been used in synthetic transformations of reactive thiols and simple alcohols,<sup>8–12</sup> where phenols were found less reactive<sup>12</sup> and TBAF-mediated reaction resulted in the OH group remaining intact.<sup>10</sup> Overall, it should be noted that standard superbasic conditions typically require a strong base, high temperature and long reaction time, which decrease the green chemistry potential of this atom-economical transformation due to lower selectivity and the formation of by-products.

In this work, we report a solid acetylene reagent CaC<sub>2</sub>/KF for the vinylation of aliphatic alcohols and phenols, which has a number of important advantages (Fig. 2). The practical application of the developed procedure allows the synthesis of important vinyl monomers as well as the late-stage vinylation of a range of complex functionalized molecules. From a fundamental point of view, the dual role of F<sup>−</sup> in the etching of the calcium carbide surface and the activation of the hydroxyl

group towards nucleophilic addition was revealed by joint experimental and theoretical studies.

## Results and discussion

For the optimization of the reaction conditions, we have chosen 3,5-dimethylphenol as a model compound for a vinylation procedure with CaC<sub>2</sub>. As expected, the reaction did not take place under regular conditions (entries 1–4, Table 1). The employment of different solvents (entries 1–3, Table 1) and bases (entry 4, Table 1) did not result in product formation. The addition of TBAF·3H<sub>2</sub>O facilitated the transformation and delivered product **2a** in 10% yield using K<sub>2</sub>CO<sub>3</sub> as a base (entry 6, Table 1). A series of experiments emphasized the key role of the F<sup>−</sup> anion in the studied vinylation reaction (entries 8–12,

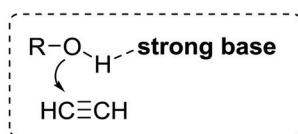
**Table 1** Optimization of reaction conditions in the vinylation of 3,5-dimethylphenol<sup>a</sup>

Entry	Solvent	Base	Additive	Yield <sup>b</sup> (%)
1	DMF	KOH	—	NR
2	Dioxane	KOH	—	NR
3	DMSO	KOH	—	NR
4	DMSO	K <sub>2</sub> CO <sub>3</sub>	—	NR
5	DMSO	KOH	TBAF·3H <sub>2</sub> O	NR
6	DMSO	K <sub>2</sub> CO <sub>3</sub>	TBAF·3H <sub>2</sub> O	10
7	DMF	K <sub>2</sub> CO <sub>3</sub>	KF	NR
8	Dioxane	K <sub>2</sub> CO <sub>3</sub>	KF	32
9	DMSO	K <sub>2</sub> CO <sub>3</sub>	KF	70
10	DMSO	K <sub>2</sub> CO <sub>3</sub>	CsF	70
11	DMSO	K <sub>2</sub> CO <sub>3</sub>	NaF	65
12	DMSO	K <sub>2</sub> CO <sub>3</sub>	LiF	50
13	DMSO	K <sub>2</sub> CO <sub>3</sub>	KCl	45
14	DMSO	K <sub>2</sub> CO <sub>3</sub>	KBr	30
15	DMSO	K <sub>2</sub> CO <sub>3</sub>	KI	21

<sup>a</sup> Conditions: **1a** (1.0 mmol), CaC<sub>2</sub> (2.0 mmol), additive (4.0 mmol), H<sub>2</sub>O (4.0 mmol), base (0.5 mmol), solvent (1.5 mL), 130 °C, 3 h.

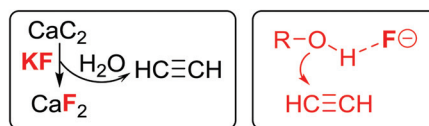
<sup>b</sup> Isolated yields.

### Known vinylation reactions



- ✗ strong bases, harsh reaction conditions, expensive metal catalysts;
- ✗ poor functional group tolerance and oligomerization side-reaction;
- ✗ high pressure of acetylene;
- ✗ dedicated expensive equipment.

### This work: CaC<sub>2</sub>/KF



- ✓ new route of F<sup>−</sup>-assisted activation;
- ✓ mild conditions without strong bases;
- ✓ usage of calcium carbide;
- ✓ regular laboratory equipment;
- ✓ late stage vinylation.

**Fig. 2** Nucleophilic addition of alcohols to acetylene: typical limitations and dual activation approach described in the present study.



Table 1), with the best results achieved using KF and CsF (entries 9 and 10, Table 1). Interestingly, other halogen anions also facilitated the reaction (entries 13–15, Table 1), although in a less efficient manner compared to F<sup>-</sup> (entry 9, Table 1).

Under optimized conditions, the reaction proceeded smoothly and gave product **2a** in 70% yield. Both KF and CsF can be used to activate CaC<sub>2</sub> in order to mediate the reaction of interest. For better cost-efficiency, further reactions were performed using KF as an additive.<sup>13</sup>

The substrate scope of the developed vinylation reaction involving calcium carbide was investigated for a number of phenols and naphthols (**2a**, **2j–2p**), substituted aliphatic alcohols (**2b–2i**), benzylic alcohol (**2q**), and functionalized biologically active and organometallic molecules **2s–2w** and **2z** (Fig. 3).

The vinylation of aliphatic and cycloaliphatic alcohols, including cyclohexanol and menthol, delivered excellent product yields (**2b–2i**). Primary as well as secondary alcohols were functionalized in the developed system in >80% yields (**2g** and **2h**).

The complete conversion and highest yield were obtained by the vinylation of *N*-methyl-2,2,6,6-tetramethyl piperidinol (**2d**). In the case of 2,2,6,6-tetramethyl piperidinol, only the

*O*-vinylated product (**2e**) was observed, as confirmed by NMR spectra (see the ESI†). In the functionalization of a highly reactive symmetrical aliphatic diol, both OH groups were vinylated (**2f**), regardless of the amount of calcium carbide added.

Among the studied phenols, the highest yield was obtained for 3,5-dimethylphenol, probably due to the favorable inductive effects of its two methyl groups (**2a**). For a similar reason, the yields with electron-rich substrates (**2a** and **2k**) were significantly higher than that of the unsubstituted phenyl vinyl ether **2l**. In the challenging case of **2p**, which contains a *p*-Cl substituent as an electron-withdrawing group, the formation of the corresponding product was still observed (*cf.* to **2a**). To confirm the influence of the electron-withdrawing group, 4-nitrophenol was studied, and indeed, no product was detected due to the reduced nucleophilicity of the corresponding alkoxide (**2r**). Even the sterically demanding *o*-Ph-substituted phenol reacted in the studied system and furnished the formation of 2-(vinyloxy)-1,1'-biphenyl (**2o**). Naphthalene derivatives represent another difficult substrate class due to their higher affinity for thermal polymerization compared to other phenyl vinyl ethers.<sup>14</sup> Nevertheless, the formation of 1-(vinyloxy)-naphthalene (**2j**) was observed in the studied system.

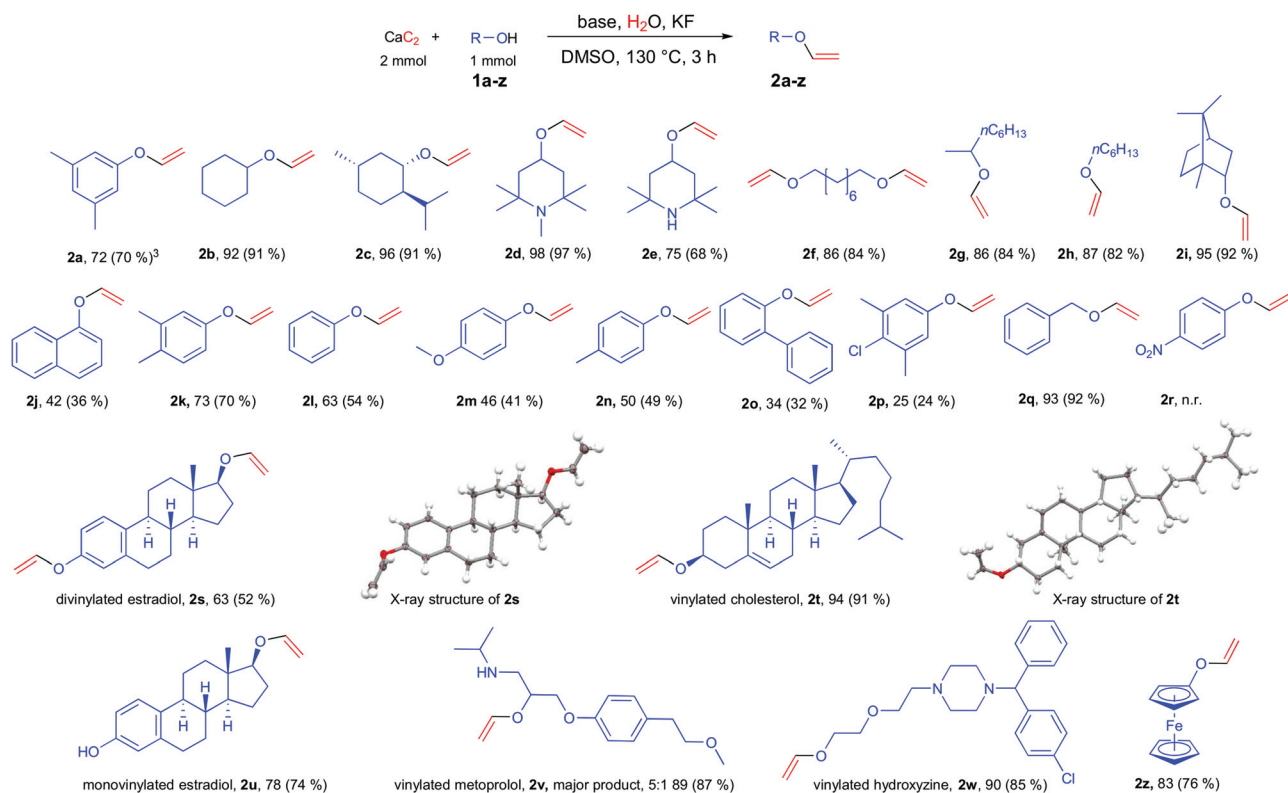


**Fig. 3** Scope of OH bond functionalization with CaC<sub>2</sub> for different substrates (experimental conditions for the synthesis of **2b–2i**, **2q** and **2z**: CaC<sub>2</sub> (2.0 mmol), substrate (1.0 mmol), KOH (1.0 mmol), KF (4.0 mmol), H<sub>2</sub>O (4.0 mmol), 130 °C, 3 h; **2a**, **2j–2p**: CaC<sub>2</sub> (2.0 mmol), substrate (1.0 mmol), K<sub>2</sub>CO<sub>3</sub> (0.5 mmol), KF (4.0 mmol), H<sub>2</sub>O (4.0 mmol), 130 °C, 3 h; **2s**, **2t**, **2v**, **2w**: CaC<sub>2</sub> (2.0 mmol), substrate (50 mg), KOH (1.0 mmol), KF (4.0 mmol), H<sub>2</sub>O (4.0 mmol); **2u**: CaC<sub>2</sub> (2.0 mmol), substrate (50 mg), KOH (1.0 mmol), H<sub>2</sub>O (4.0 mmol); freshly powdered calcium carbide was used in all cases. NMR yields and isolated yields (in parenthesis) are shown; for compounds **2j–2n** modified sequential vinylation was applied to improve isolated yields (see the ESI† for details); for **2f** the amount of substrate was 0.5 mmol. Single-crystal X-ray structures of **2s** and **2t** are shown.



The efficiency of this process allowed for the direct vinylation of OH-containing pharmacologically active substances, such as steroids and drugs, in good to high yields. Again, the crucial role of fluoride is reflected in the vinylation of estradiol. Using KF as an additive, estradiol was vinyated at both OH groups, delivering the corresponding divinylated estradiol (**2s**) in good yield. In the absence of KF, the process provides solely the monovinylated product **2u** with an aliphatic *O*-vinyl ether group. The structure of **2u** was confirmed by HMBC and NOESY experiments, and the structures of **2s** and **2t** were confirmed by NMR and X-ray analyses (Fig. 3). The treatment of cholesterol with  $\text{CaC}_2$  gave the vinylation product in a 91% isolated yield (**2t**).

To further explore the possibilities of late-stage functionalization, we also vinyated metoprolol (a selective  $\beta_1$  receptor blocker, marketed under the trade name Lopressor®)<sup>15</sup> and hydroxyzine (a tranquilizer, marketed as Atarax®).<sup>16</sup> Hydroxyzine was vinyated with  $\text{CaC}_2$ , and the corresponding product was isolated in 85% yield (**2w**). Metoprolol was vinyated with  $\text{CaC}_2$  at both oxygen and nitrogen atoms with an 89% overall yield and a good 5:1 selectivity between the *O*-vinyated product **2v** and *N*-vinyated product. The structure of **2v** was confirmed by HMBC, HMQC and NOESY experiments.

The key advantage of the developed system is the utilization of transition metal free inorganic reagents ( $\text{CaC}_2$ , KF and inorganic base  $\text{K}_2\text{CO}_3$  or KOH) and water to carry out the transformation. Thus, a simplified reaction set-up and an easy

product separation were possible. In most of the studied cases, product losses were minimized, so that a small difference between the NMR yields and isolated yields was observed (Fig. 3).

To reveal the reaction mechanism we have first confirmed the involvement of acetylene in the studied system. The reaction was carried out using gaseous acetylene (instead of  $\text{CaC}_2$ ) and the formation of the vinylation product was observed in the presence of KF/ $\text{K}_2\text{CO}_3$ . To confirm the proposed mechanistic assumption we have also detected acetylene *in situ* in the reaction with  $\text{CaC}_2$ . The reaction was carried out in the NMR tube and acetylene was detected in the  $^1\text{H}$  NMR spectrum which is in total agreement with the proposed mechanism. In addition, carrying out the reaction with  $\text{D}_2\text{O}$  (instead of  $\text{H}_2\text{O}$ ) in  $\text{DMSO-d}_6$  resulted in >80% incorporation of deuterium in the vinylation product (approximate ratio of D:H ~ 5:1 in the vinyl groups). This experiment required the preliminary conversion of the ROH substrate to ROD to avoid deuterium scrambling (the presence of residual exchangeable protons in the substrate and base leads to some amount of the non-deuterated product).

It is of great interest to reveal the nature of the activating effect of the fluorine anion. In the first step, it is expected that the reaction of  $\text{CaC}_2$  with water generates acetylene and is accompanied by the formation of  $\text{Ca}(\text{OH})_2$  as an inorganic phase. Unexpectedly, the experiment showed that the inorganic component was precipitated as insoluble calcium fluo-

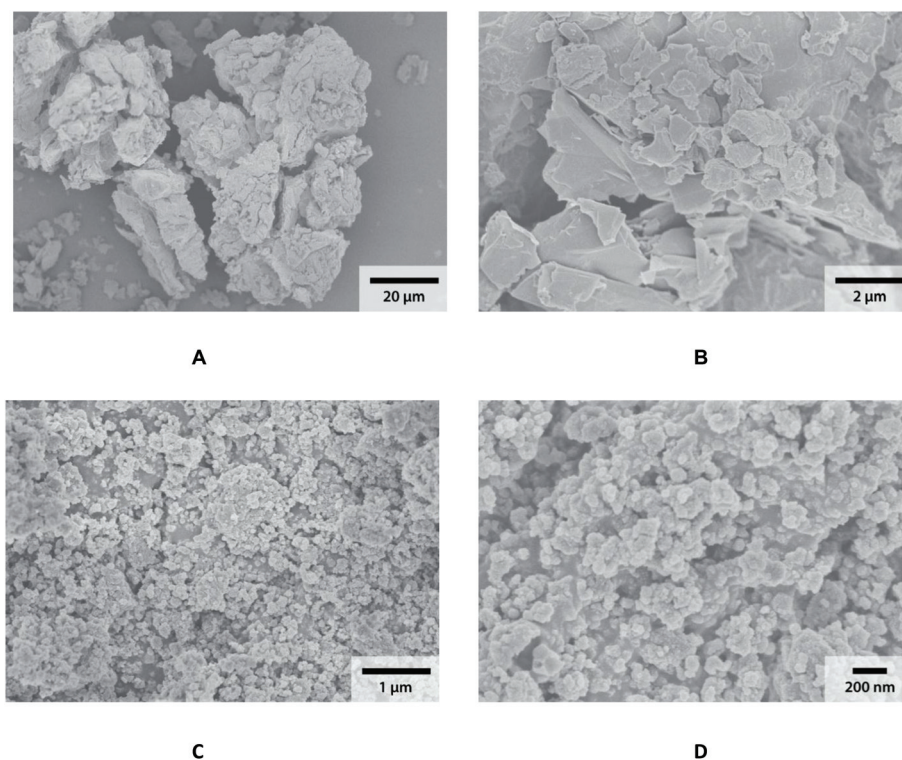


Fig. 4 Scanning electron microscopy images of initial calcium carbide (A and B) and the inorganic residue isolated after the reaction (C and D), shown at low (A), medium (B, C) and high (D) magnifications.



ride after the reaction (Fig. 4). To trace the transformations of calcium carbide, the solid residue in the model reaction of the vinylation of 3,5-dimethylphenol was subjected to field-emission scanning electron microscopy (FE-SEM) and EDS analyses. Electron microscopy showed that the calcium carbide initially consisted of aggregated flaky particles with characteristic sizes of approximately several micrometers for individual particles and tens of micrometers for aggregates (Fig. 4A and 4B). After the reaction, the morphology of the solid phase isolated from the reaction mixture changed drastically. The particles had a nearly round shape and sizes from several tens to hundreds of nanometers (Fig. 4A and 4B). X-ray microanalysis by EDS-SEM and X-ray powder diffraction (XPD) studies confirmed the transition of fluorine from solution into the solid phase and the formation of  $\text{CaF}_2$  (see the ESI†). The analysis of the solid sample isolated after the reaction showed that approximately 90–95% of the calcium in the studied sample existed in the form of  $\text{CaF}_2$ .<sup>17</sup>

This finding can be rationalized by taking into account the difference in solubility:  $1.73 \text{ g L}^{-1}$  for  $\text{Ca(OH)}_2$  and only  $0.016 \text{ g L}^{-1}$  for  $\text{CaF}_2$  (in water).<sup>18</sup> Because solubility data in DMSO were not available, we carried out two control experiments to confirm the nature of the process. First, a mixture of  $\text{Ca(OH)}_2$  and KF was heated in DMSO for 3 h. Indeed,  $\text{Ca(OH)}_2$  was completely converted into  $\text{CaF}_2$  upon the reaction with KF in DMSO (eqn (1), Fig. 5). To model the reaction conditions, a three-component mixture with  $\text{CaC}_2$  was studied and showed the formation of  $\text{CaF}_2$  as a solid precipitate (eqn (2), Fig. 5).

These findings highlight one of the key roles of  $\text{F}^-$  in the studied system. Under standard conditions (without  $\text{F}^-$ ), the reaction of solid particles of  $\text{CaC}_2$  with water leads to the coverage of the calcium carbide particle surface with amorphous  $\text{Ca(OH)}_2$ . The presence of fluoride anions results in a continuous etching on the surface of  $\text{CaC}_2$ , leading to an efficient surface renewal and a controllable rate of acetylene evolution. The conversion to crystalline  $\text{CaF}_2$  prevents the coverage of the carbide particles with amorphous calcium hydroxide.

However, the role of fluoride is not limited to the solid-state process. We carried out a set of control experiments under 1 atm acetylene pressure for 3,5-dimethylphenol and benzyl alcohol (the reaction was carried out using gaseous acetylene instead of  $\text{CaC}_2$ ). In the absence of KF, 3,5-dimethylphenol did not react with acetylene, while in the presence of KF, the formation of the vinylation product was detected. The more reactive benzyl alcohol reacted with acetylene in the absence of KF, although a higher yield was obtained in the presence of KF.

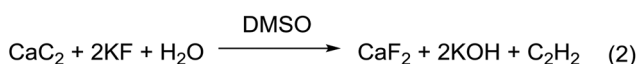
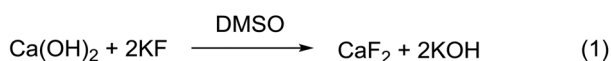


Fig. 5 Fluoride-mediated activation of calcium carbide: formation of  $\text{CaF}_2$  in two- and three-component reactions with KF in DMSO.

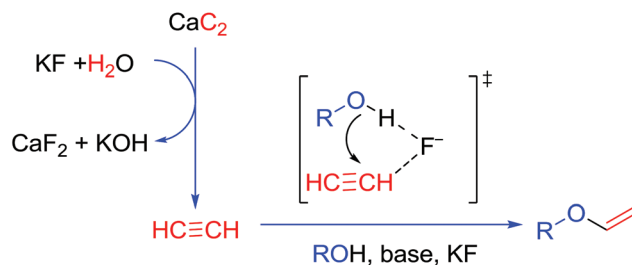


Fig. 6 Plausible mechanism for the vinylation of alcohols and phenols in the  $\text{CaC}_2/\text{KF}$  system.

Therefore, the presence of the fluoride anion also facilitates the reaction between acetylene and the hydroxyl group in solution (in addition to the transformation of inorganic components into calcium fluoride).

The overall mechanism would involve the generation of acetylene by the reaction of calcium carbide with  $\text{KF}/\text{H}_2\text{O}$  as an initial step (Fig. 6). Next, the nucleophilic addition of the hydroxyl group to the triple bond of the alkyne may be further enhanced by the formation of an intermediate complex involving the fluoride anion. The complexes and clusters between halogen anions and acetylene are known, and hydrogen bonding between fluoride anions and a relatively acidic acetylenic proton may also be anticipated in aprotic media.<sup>19,20</sup> The interaction of  $\text{F}^-$  with alcohols has been reported and applied in sensor applications.<sup>21</sup> In this case, an intermediate complex would geometrically pre-activate the substrates towards the desired addition reaction (Fig. 6) as well as enhance the reactivity *via* electron density delocalization. If the assumption is correct, then larger and less electronegative halogen atoms ( $\text{Cl}^-$ ,  $\text{Br}^-$  and  $\text{I}^-$ ) may also exhibit a similar effect, although to a lesser extent. Indeed, the observed experimental findings are in good agreement with the proposed mechanism (entries 9 and 13–15; Table 1).

To reveal the nature of the observed activating effect of the fluoride anion, we carried out a series of theoretical calculations at the CCSD(T)/6-311++G(d,p) level and accounted for the DMSO solvent effect with the SMD method (Fig. 7 and 8). A direct reaction of an alcohol ( $\text{ROH}$ ,  $\text{R} = \text{CH}_3$  for model system) with the triple bond of acetylene ( $\text{I} \rightarrow \text{II-TS} \rightarrow \text{III}$ ) requires overcoming a high activation barrier of  $\Delta E^\ddagger = 48.6 \text{ kcal mol}^{-1}$  (Fig. 7A).

Theoretical calculations have shown that both reagents ( $\text{ROH}$  and acetylene) indeed do coordinate to the fluoride anion (Fig. 7). Hydrogen bonding with the hydroxyl group and the acetylenic proton resulted in the formation of the linear intermediate complex **I-F**. Starting from the compound **I-F**, a computational study has revealed two possible pathways (Fig. 7B): (1) the reaction with the fluoride anion remaining coordinated to the acetylenic proton (**II-TS-F**); and (2) the reaction involving the interaction of the fluoride anion with the hydroxyl group (**IV-TS-F**). In the first case, the activation barrier of the **I-F**  $\rightarrow$  **II-TS-F**  $\rightarrow$  **III-F** transformation was increased to  $\Delta E^\ddagger = 55.4 \text{ kcal mol}^{-1}$ , reflecting an increase in



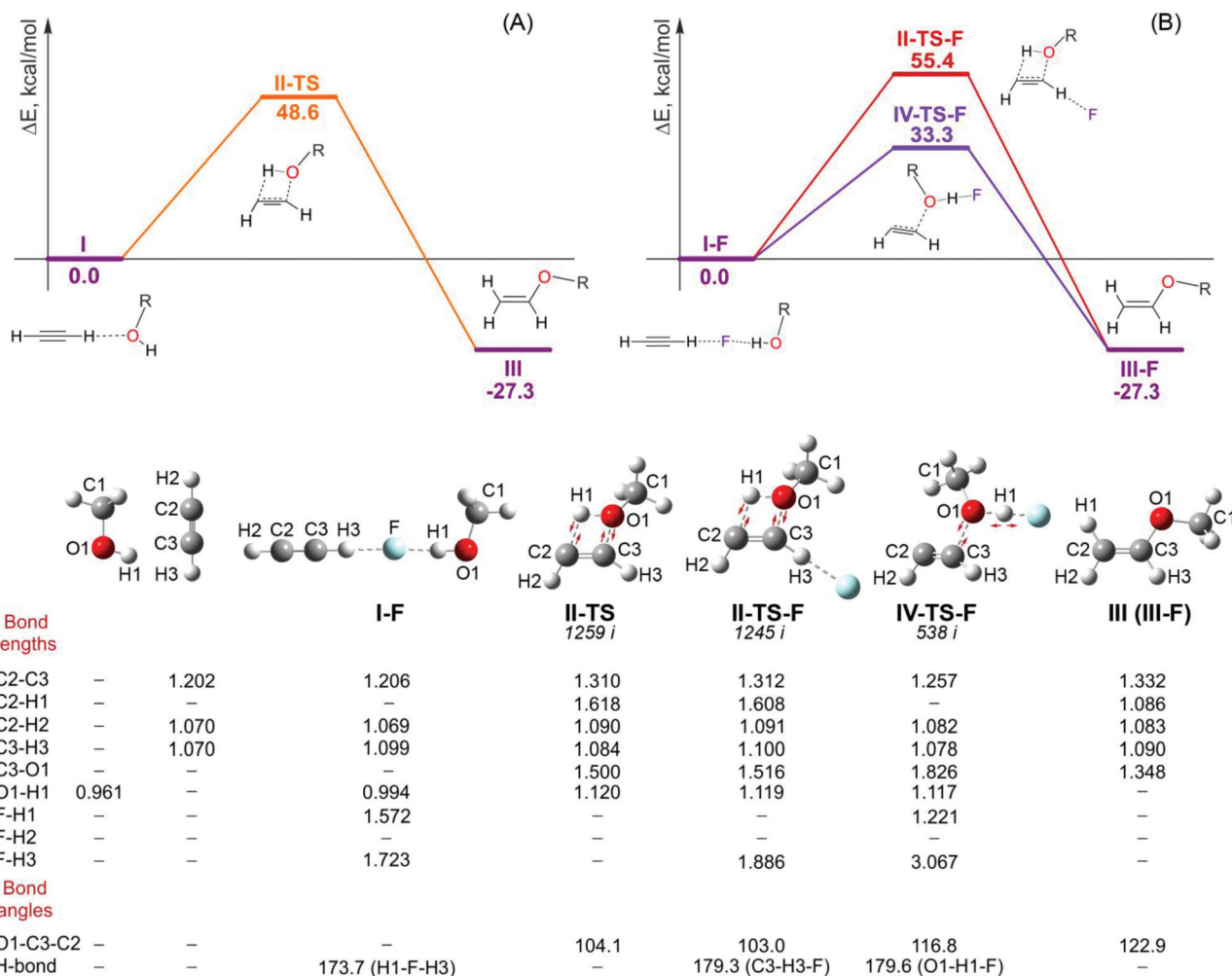


Fig. 7 Mechanistic studies with theoretical calculations: (A) hydroxyl group addition to acetylene and (B) fluoride-mediated hydroxyl group addition to acetylene (energy calculations at the CCSD(T)/6-311++G(d,p) level, geometry optimization at the PBE1PBE/6-311++G(d,p) level, and solvent effect accounted for at the SMD level;<sup>22</sup> for a visual comparison of activation barriers, the energies of I and I-F were set to 0.0 kcal mol<sup>-1</sup> on the potential energy surfaces (A) and (B); the energy changes  $\Delta E = -40.8$  kcal mol<sup>-1</sup> for isolated molecules and  $-8.2$  for DMSO medium were calculated for the reaction:  $I + F^- \rightarrow I-F$  (Fig. S5 and S6<sup>†</sup>); the fluoride-containing anion I-F is regenerated at point III-F by reaction of F<sup>-</sup> with I. See the ESI<sup>†</sup> for the details.

the negative charge of the alkyne unit, which hampered nucleophilic addition.

Remarkably, the hydrogen bonding between the hydroxyl group and the fluoride anion greatly reduces the activation barrier of the  $I-F \rightarrow IV-TS-F \rightarrow III-F$  transformation to  $\Delta E^\ddagger = 33.3$  kcal mol<sup>-1</sup>, likely because of an increase in the nucleophilicity of the oxygen atom. The overall process is exothermic by  $\Delta E^\ddagger = -27.3$  kcal mol<sup>-1</sup> (Fig. 7B). The same conclusions were made upon the analysis of the  $\Delta H$  and  $\Delta G$  energy surfaces.<sup>22</sup> We also carried out the theoretical modeling of the process involving Cl<sup>-</sup> instead of F<sup>-</sup> and found the calculated energy barrier for the  $I-Cl \rightarrow IV-TS-Cl \rightarrow III-Cl$  transformation to be  $\Delta E^\ddagger = 37.1$  kcal mol<sup>-1</sup>. The results agree with the experimental findings, where the activating effect of the chloride anion was observed to be noticeably less than that of the fluoride anion (Table 1).

After studying a small model system, the calculations involving phenol as a substrate were carried out using the same theory level (the CCSD(T)/6-311++G(d,p) level for energy and the SMD method to account for the DMSO solvent effect). The calculated energy surfaces have revealed the key trends of the investigated vinylation process (Fig. 8). The direct reaction between phenol and acetylene ( $I \rightarrow II-TS \rightarrow III$ ) required overcoming a much larger activation barrier  $\Delta E^\ddagger = 57.5$  kcal mol<sup>-1</sup> (Fig. 8A) as compared to the aliphatic alcohol  $\Delta E^\ddagger = 48.6$  kcal mol<sup>-1</sup> (Fig. 7A). Optimized geometries showed more efficient interaction of the RO group with an acetylene carbon atom in the case of the R = Me substituent as compared with the R = Ph substituent in the transition state **II-TS** (the C3-O1 distance is 1.500 Å for R = Me and 2.076 Å for R = Ph). The results are in agreement with experimental findings, where a lower reactivity of phenols as com-



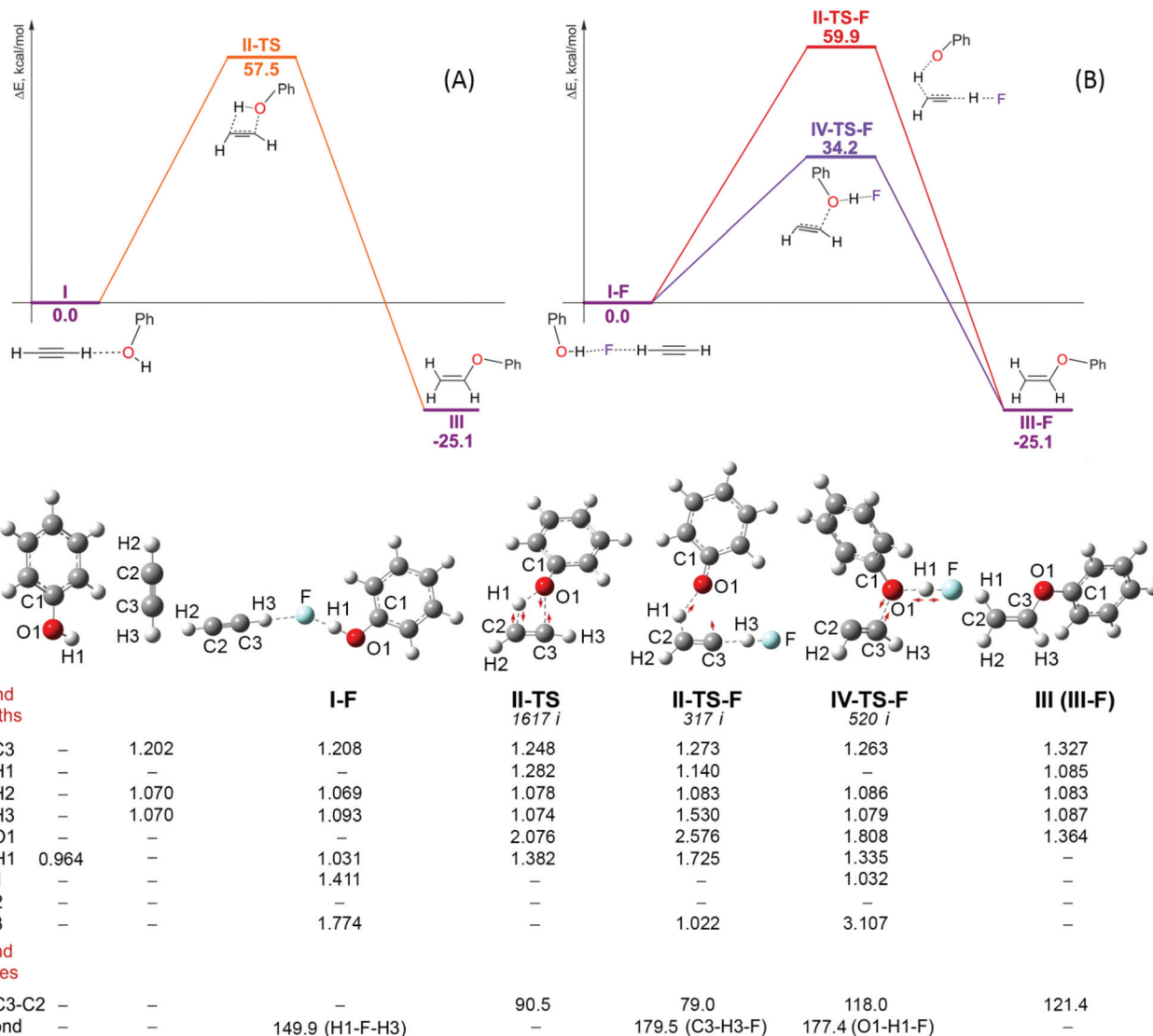


**Fig. 8** Mechanistic studies of acetylene vinylation with phenol using theoretical calculations: (A) addition of a hydroxyl group of phenol to acetylene and (B) fluoride-mediated addition of a hydroxyl group of phenol to acetylene (energy calculations at the CCSD(T)/6-311++G(d,p) level, geometry optimization at the PBE1PBE/6-311++G(d,p) level, and the solvent effect accounted for at the SMD level; the energies of I and I-F were set to 0.0 kcal mol<sup>-1</sup> for comparative purposes similar to the previous reaction, see caption to Fig. 7).

pared to aliphatic alcohols was observed. The fluoride-mediated activation of the hydroxyl group significantly decreased the barrier height to  $\Delta E^\ddagger = 34.2$  kcal mol<sup>-1</sup> for the I-F  $\rightarrow$  IV-TS-F  $\rightarrow$  III-F pathway (Fig. 8B). Thus, fluoride-mediated activation makes the process feasible under studied conditions in total agreement with the experimental observations.

Of course, the computational study deals with a model system and may be subject to some limitations in accuracy. Nevertheless, the calculated energy surfaces and the revealed relative trends clearly confirm the advantage of the F<sup>-</sup>-mediated addition of the hydroxyl group to an alkyne. The unique nature of fluoride substantially reduced the energy barrier and facilitated the transformation of interest.

## Conclusions

To summarize, we have developed an efficient procedure for the preparation of vinyl ethers from alcohols and phenols using a simple CaC<sub>2</sub>/KF system. The procedure allows the direct and cost-efficient formation of important H<sub>2</sub>C=CH-O building blocks under easy to use conditions (without the involvement of high pressure acetylene). Two areas of application have been explored in the present study. First, important vinylic monomers of aliphatic and aromatic alcohols have been synthesized (2a–2q), which are of much interest for materials science and industrial applications. Second, mild experimental conditions and a high functional tolerance make the methodology suitable for the post-modification of complex



biologically active molecules and drugs (**2s–2w**) using calcium carbide as an easily available reagent. The developed approach provides a new methodology for the vinylation of biologically active molecules and pharmaceutical substances, leading to the formation of highly demanded vinyl ethers. These products are of great interest for the preparation of well-defined and multifunctional drug-containing polymers.

Two fundamentally important findings were revealed in the present study: the etching of the calcium carbide surface by the fluoride ions and the fluoride-mediated activation of alcohols for the nucleophilic transformations. A combination of  $\text{CaC}_2/\text{KF}$  can be considered as an efficient replacement of high-pressure gaseous acetylene, which is difficult to handle in the laboratory. Moreover, the usage of  $\text{CaC}_2/\text{KF}$  as an acetylene surrogate demonstrated enhanced reactivity of the  $\text{C}\equiv\text{C}$  bond. A mechanistic study involving theoretical calculations has shown a significant decrease of the activation barrier of the vinylation reaction in the fluoride-mediated process.

Undoubtedly, these novel findings will open several new opportunities in synthetic transformations. The application of an easy to weigh and handle solid “acetylene reagent” (a combination of  $\text{CaC}_2$  and  $\text{KF}$ ) may introduce a new direction in the well-known and powerful acetylene chemistry.

## Experimental part

### A typical procedure for the vinylation of phenols (synthesis of **2a**, **2j–2p**, **2z**)

$\text{K}_2\text{CO}_3$  (0.5 mmol, 69 mg), alcohol (1.0 mmol),  $\text{KF}$  (4.0 mmol, 232 mg) and freshly powdered calcium carbide (2.0 mmol, 128 mg) were added to a reaction tube (7 mL) with 1.5 mL of dry DMSO. After stirring at room temperature for 5 min, water (4.0 mmol, 72  $\mu\text{L}$ ) was added, the tube was sealed, and the mixture was heated at 130 °C for 3 h with vigorous stirring. After cooling to 25 °C, the mixture was extracted with hexane (3  $\times$  4 mL), and the collected hexane layers were concentrated under reduced pressure (see Fig. 3 for the yields).

### A typical procedure for the vinylation of aliphatic and benzylic alcohols (synthesis of **2b–2i** and **2q**)

$\text{KOH}$  (1.0 mmol, 69 mg), alcohol (1.0 mmol),  $\text{KF}$  (4.0 mmol, 232 mg) and freshly powdered calcium carbide (2.0 mmol, 128 mg) were added to a reaction tube (7 mL) with 1.5 mL of dry DMSO. After stirring at room temperature for 5 min, water (4.0 mmol, 72  $\mu\text{L}$ ) was added, the tube was sealed, and the mixture was heated at 130 °C for 3 h with vigorous stirring. After cooling to 25 °C, the mixture was extracted with hexane (3  $\times$  4 mL), and the collected hexane layers were concentrated under reduced pressure (see Fig. 3 for the yields).

### Scaling of the experimental procedure

The procedure was successfully scaled to synthesize 2.72 g of product **2q** in a single run in 70% yield (see the ESI† for details).

### A typical procedure for the vinylation of biologically active molecules (for the synthesis of **2s**, **2t**, **2v** and **2w**)

$\text{KOH}$  (2.0 mmol, 112 mg), substrate (50 mg),  $\text{KF}$  (4.0 mmol, 232 mg) and freshly powdered calcium carbide (2.0 mmol, 128 mg) were added to a reaction tube (volume: 7 mL) with 1.5 mL of dry DMSO. After stirring the mixture at room temperature for 5 min, water (4.0 mmol, 72  $\mu\text{L}$ ) was added. The tube was sealed, and the mixture was heated at 130 °C for 3 h with vigorous stirring. The reaction mixture was cooled to 25 °C and extracted with hexane (3  $\times$  4 mL), and the collected hexane layers were dried under vacuum to give a pure product (see Fig. 3 for the yields).

### Monovinylation of estradiol

$\text{KOH}$  (2.0 mmol, 112 mg), estradiol (50 mg), and freshly powdered calcium carbide (2.0 mmol, 128 mg) were added to a reaction tube (volume: 7 mL) with 1.5 mL of dry DMSO. After stirring the mixture at room temperature for 5 min, water (4.0 mmol, 72  $\mu\text{L}$ ) was added. The tube was sealed, and the mixture was heated at 130 °C for 3 h with vigorous stirring. The reaction mixture was cooled to 25 °C and extracted with hexane (3  $\times$  4 mL), purified with chromatography and dried under vacuum to give a pure product. Estradiol monovinyl ether (**2u**) was obtained as white crystals (45 mg, 74%).

### Further purification of the products

Typically, after evaporation of hexane the vinylated products were obtained in high purity (see the ESI†). For further purification, if required, the products can be distilled under reduced pressure. In general, purification *via* column chromatography on silica is not suggested due to sensitivity of the vinyl ethers towards undergoing rapid polymerization or degradation (some products are stable, however, and can be purified by chromatography, see the ESI†). Several vinyl ethers become highly unstable in the pure form upon drying and undergo fast polymerization, such products may be stabilized by dilution with pentane or hexane and stored in solution.

### Electron microscopy study

Before the measurements, the samples were mounted on a 25 mm aluminum specimen stub and fixed by conductive double-sided tape. Coating with a thin film (10 nm) of palladium was performed using the magnetron sputtering method. The observations were carried out using a Hitachi SU8000 field-emission scanning electron microscope (FE-SEM). Images were acquired in the secondary electron mode at a 2 kV accelerating voltage and a working distance of 4–5 mm. The morphology of the coated samples was studied, adjusting for the metal coating surface effects. EDS-SEM studies were carried out using an Oxford Instruments X-max EDX system, with spectra acquired at a 10 kV accelerating voltage. For the quantitative analysis, internal standards were used. Before the measurements, all samples were coated with a thin film (15 nm) of carbon using a Cressington 208 carbon coater.





## Computational study

For all optimized structures, single-point CCSD(T)<sup>23</sup> calculations involving the 6-311++G(d,p) basis set were performed in a vacuum and in DMSO (the SMD method to account for the effect of the solvent). All structures were optimized by the PBE1PBE<sup>24</sup> DFT method with the 6-311++G(d,p) basis set<sup>25</sup> (Grid = UltraFine). Calculations in DMSO medium were performed by the SMD continuum solvation model.<sup>26</sup> Molecular structures were optimized in DMSO medium. For all molecules, the normal mode analysis was carried out at the DFT level, and all transition states have one imaginary frequency corresponding to the hydroalkoxylation reaction. The validity of all transition states was confirmed by intrinsic reaction coordinate (IRC) calculations.<sup>27</sup> Only the essential narrative of the calculated data is discussed in the article, see the ESI† for details. The Gaussian 09 program was used for all calculations.<sup>28</sup>

## Competing financial interests

The authors declare no competing financial interests.

## Acknowledgements

Synthetic studies were supported by the Russian Science Foundation (grant 16-13-10301). GW acknowledges Saint Petersburg State University for a postdoctoral fellowship (No 0.50.1186.2014). The authors also express their gratitude to the Centre for Magnetic Resonance, X-ray Diffraction Center, the Centre for Chemical Analysis and Materials Research and the Interdisciplinary Center for Nanotechnology (Saint Petersburg State University). Mechanistic studies using theoretical calculations and microscopy were supported by Russian Science Foundation (RSF grant 14-50-00126). The authors thank Dr Yan Zubavichus and Victor Khurstalev for carrying out XPD analysis.

## References

- 1 Representative examples: (a) T. Cernak, K. D. Dykstra, S. Tyagarajan, P. Vachal and S. W. Krska, *Chem. Soc. Rev.*, 2016, **45**, 546; (b) J. Wencel-Delord and F. Glorius, *Nat. Chem.*, 2013, **5**, 369; (c) P. A. Wender and J. L. Baryza, *Org. Lett.*, 2005, **7**, 1177.
- 2 (a) T. Krasia-Christoforou and T. K. Georgiou, *J. Mater. Chem. B*, 2013, **1**, 3002; (b) B. T. Luk, R. H. Fang and L. Zhang, *Theranostics*, 2012, **2**, 1117; (c) A. Puri and R. Blumenthal, *Acc. Chem. Res.*, 2011, **44**, 1071; (d) Z. Wang, G. Niu and X. Chen, *Pharm. Res.*, 2013, **31**, 1358; (e) X. Li, Y. Qian, T. Liu, X. Hu, G. Zhang, Y. You and S. Liu, *Biomaterials*, 2011, **32**, 6595; (f) Y. Liu, L. Feng, T. Liu, L. Zhang, Y. Yao, D. Yu, L. Wang and N. Zhang, *Nanoscale*, 2014, **6**, 3231; (g) C.-Y. Hsu, M.-P. Nieh and P.-S. Lai, *Chem. Commun.*, 2012, **48**, 9343; (h) S. Wang, G. Kim, Y.-E. K. Lee, H. J. Hah, M. Ethirajan, R. K. Pandey and R. Kopelman, *ACS Nano*, 2012, **6**, 6843; (i) R. Duncan, *Curr. Opin. Biotechnol.*, 2011, **22**, 492; (j) C. Fu, A. Bongers, K. Wang, B. Yang, Y. Zhao, H. Wu, Y. Wei, H. T. T. Duong, Z. Wang and L. Tao, *Polym. Chem.*, 2016, **7**, 546.
- 3 (a) M. Ouchi, M. Kamigaito and M. Sawamoto, *Macromolecules*, 1999, **32**, 6407; (b) Y. Hirokawa, T. Higashimura, K. Matsuzaki and T. Uryu, *J. Polym. Sci., Polym. Chem. Ed.*, 1979, **17**, 1473; (c) T. Kawaguchi, F. Sanda and T. Masuda, *J. Polym. Sci., Part A: Polym. Chem.*, 2002, **40**, 3938.
- 4 W. Reppe, *Justus Liebigs Ann. Chem.*, 1956, **601**, 81.
- 5 Selected recent reviews: (a) B. M. Trost and C.-J. Li, *Modern Alkyne Chemistry: Catalytic and Atom-Economic Transformations*, Wiley-VCH, Weinheim, 2015; (b) R. Salvio, M. Moliterno and M. Bella, *Asian J. Org. Chem.*, 2014, **3**, 340; (c) W. Wu and H. Jiang, *Acc. Chem. Res.*, 2014, **47**, 2483; (d) R. Chinchilla and C. Nájera, *Chem. Rev.*, 2014, **114**, 1783; (e) S. A. Vizer, E. S. Sycheva, A. A. A. Al Quntar, N. B. Kurmankulov, K. B. Yerzhanov and V. M. Dembitsky, *Chem. Rev.*, 2015, **115**, 1475; (f) F. Klappenberger, Y.-Q. Zhang, J. Björk, S. Klyatskaya, M. Ruben and J. V. Barth, *Acc. Chem. Res.*, 2015, **48**, 2140; (g) I.-T. Trotsuş, T. Zimmermann and F. Schüth, *Chem. Rev.*, 2014, **114**, 1761; (h) F. Diederich, P. J. Stang and R. R. Tykwinski, *Acetylene Chemistry. Chemistry, Biology and Material Science*, Wiley-VCH Verlag GmbH & Co. KGaA, Weinheim, 2005; (i) P. J. Stang and F. Diederich, *Modern Acetylene Chemistry*, Wiley-VCH Verlag GmbH & Co. KGaA, Weinheim, 2008.
- 6 Addition to alkynes under “super-basic” conditions: (a) R. K. Sharma and J. L. Fry, *J. Org. Chem.*, 1983, **48**, 2112; (b) C. L. Liotta and H. P. Harris, *J. Am. Chem. Soc.*, 1974, **96**, 2250; (c) R. A. Bartsch, *J. Org. Chem.*, 1970, **35**, 1023; (d) J. Emsley, D. J. Jones, J. M. Miller, R. E. Overill and R. A. Waddilove, *J. Am. Chem. Soc.*, 1981, **103**, 24; (e) L. A. Oparina, M. Y. Khil’ko, N. A. Chernyshova, S. I. Shaikhudinova, L. N. Parshina, T. Preiss, J. Henkelmann and B. A. Trofimov, *Russ. J. Org. Chem.*, 2005, **41**, 661; (f) L. A. Oparina, S. I. Shaikhudinova, L. N. Parshina, O. V. Vysotskaya, T. Preiss, J. Henkelmann and B. A. Trofimov, *Russ. J. Org. Chem.*, 2005, **41**, 656.
- 7 Alkynes as universal building blocks: K. I. Galkin and V. P. Ananikov, *Russ. Chem. Rev.*, 2016, **85**, 226.
- 8 See review: K. S. Rodygin, G. Werner, F. A. Kucherov and V. P. Ananikov, *Chem. – Asian J.*, 2016, **11**, 965, (and references therein).
- 9 CaC<sub>2</sub> is an important commodity chemical with an annual production >20 million tons that is available in different crystal modifications: S. Konar, J. Nylén, G. Svensson, D. Bernin, M. Edén, U. Ruschewitz and U. Häussermann, *J. Solid State Chem.*, 2016, **239**, 204.
- 10 A. Hosseini, D. Seidel, A. Miska and P. R. Schreiner, *Org. Lett.*, 2015, **17**, 2808.
- 11 (a) K. S. Rodygin and V. P. Ananikov, *Green Chem.*, 2016, **18**, 482; (b) K. S. Rodygin, A. A. Kostin and V. P. Ananikov, *Mendeleev Commun.*, 2015, **25**, 415.



- 12 (a) R. Matake, Y. Adachi and H. Matsubara, *Green Chem.*, 2016, **18**, 2614; (b) S. P. Teong, A. Y. H. Chua, S. Deng, X. Li and Y. Zhang, *Green Chem.*, 2017, **19**, 1659.
- 13 Comparison of cost: KF, CAS 7789-23-3, Sigma-Aldrich, 50 € per 250 g; CsF, CAS 13400-13-0, Sigma-Aldrich, 276 € per 100 g (accessed on March 2017). As an estimate only, since the price may depend on many factors.
- 14 B. A. Trofimov, L. A. Oparina, N. A. Kolyvanov, O. V. Vysotskaya and N. K. Gusarova, *Russ. J. Org. Chem.*, 2014, **55**, 188.
- 15 (a) M. L. Fisher, S. S. Gottlieb, G. D. Plotnick, N. L. Greenberg, R. D. Patten, S. K. Bennett and B. P. Hamilton, *J. Am. Coll. Cardiol.*, 1994, **23**, 943; (b) P. Fletcher and J. Hunter, *Aust. Prescr.*, 2000, **23**, 120.
- 16 H. M. Robinson, R. C. Robinson and J. F. Strahan, *South. Med. J.*, 1957, **50**, 1282.
- 17 For statistical averaging, several experiments involving 3,5-dimethylphenol and benzyl alcohol as substrates were carried out, and the content of CaF<sub>2</sub> of 90–95% is based on 12 independent measurements.
- 18 P. Patnaik, *Handbook of Inorganic Chemicals*, McGraw-Hill, 2002.
- 19 (a) P. S. Weiser, D. A. Wild and E. J. Bieske, *J. Chem. Phys.*, 1999, **110**, 9443; (b) D. A. Wild, Z. M. Loh and E. J. Bieske, *Aust. J. Chem.*, 2011, **64**, 633.
- 20 J. Emsley, *Chem. Soc. Rev.*, 1980, **9**, 91.
- 21 (a) D. W. Kim, Hwan-Jeong, S. T. Lim, M.-H. Sohn, J. A. Katzenellenbogen and D. Y. Chi, *J. Org. Chem.*, 2008, **73**, 957; (b) D. W. Kim, H.-J. Jeong, S. T. Lim and M.-H. Sohn, *Tetrahedron Lett.*, 2010, **51**, 432; (c) V. F. DeTuri, M. A. Su and K. M. Ervin, *J. Phys. Chem. A*, 1999, **103**, 1468; (d) V. F. DeTuri and K. M. Ervin, *J. Phys. Chem. A*, 1999, **103**, 6911; (e) B. Bogdanov and T. B. McMahon, *J. Phys. Chem. A*, 2000, **104**, 7871; (f) D. A. Jose, P. Kar, D. Koley, B. Ganguly, W. Thiel, H. N. Ghosh and A. Das, *Inorg. Chem.*, 2007, **46**, 5576; (g) S. Verma, S. Aute, A. Das and H. N. Ghosh, *J. Phys. Chem. B*, 2015, **119**, 14952; (h) X. Zhang, J. Fu, T.-G. Zhan, L. Dai, Y. Chen and X. Zhao, *Tetrahedron Lett.*, 2013, **54**, 5039; (i) C.-H. Chen and M.-k. Leung, *Tetrahedron*, 2011, **67**, 3924.
- 22 Only selected structures and parameters are discussed in the article, see the ESI† for details and additional data on theoretical calculations.
- 23 (a) R. J. Bartlett and G. D. Purvis, *Int. J. Quantum Chem.*, 1978, **14**, 561; (b) J. A. Pople, R. Krishnan, H. B. Schlegel and J. S. Binkley, *Int. J. Quantum Chem.*, 1978, **14**, 545; (c) J. A. Pople, M. Head-Gordon and K. Raghavachari, *J. Chem. Phys.*, 1987, **87**, 5968; (d) R. J. Bartlett and M. Musiał, *Rev. Mod. Phys.*, 2007, **79**, 291.
- 24 (a) J. P. Perdew, K. Burke and M. Ernzerhof, *Phys. Rev. Lett.*, 1996, **77**, 3865; (b) C. Adamo and V. Barone, *J. Chem. Phys.*, 1999, **110**, 6158.
- 25 (a) A. D. McLean and G. S. Chandler, *J. Chem. Phys.*, 1980, **72**, 5639; (b) R. Krishnan, J. S. Binkley, R. Seeger and J. A. Pople, *J. Chem. Phys.*, 1980, **72**, 650; (c) T. Clark, J. Chandrasekhar, G. W. Spitznagel and P. V. R. Schleyer, *J. Comput. Chem.*, 1983, **4**, 294.
- 26 A. V. Marenich, C. J. Cramer and D. G. Truhlar, *J. Phys. Chem. B*, 2009, **113**, 6378.
- 27 H. P. Hratchian and H. B. Schlegel, *J. Chem. Theory Comput.*, 2005, **1**, 61.
- 28 M. J. Frisch, G. W. Trucks, H. B. Schlegel, G. E. Scuseria, M. A. Robb, J. R. Cheeseman, G. Scalmani, V. Barone, B. Mennucci, G. A. Petersson, H. Nakatsuji, M. Caricato, X. Li, H. P. Hratchian, A. F. Izmaylov, J. Bloino, G. Zheng, J. L. Sonnenberg, M. Hada, M. Ehara, K. Toyota, R. Fukuda, J. Hasegawa, M. Ishida, T. Nakajima, Y. Honda, O. Kitao, H. Nakai, T. Vreven, J. A. Montgomery Jr., J. E. Peralta, F. Ogliaro, M. Bearpark, J. J. Heyd, E. Brothers, K. N. Kudin, V. N. Staroverov, T. Keith, R. Kobayashi, J. Normand, K. Raghavachari, A. Rendell, J. C. Burant, S. S. Iyengar, J. Tomasi, M. Cossi, N. Rega, J. M. Millam, M. Klene, J. E. Knox, J. B. Cross, V. Bakken, C. Adamo, J. Jaramillo, R. Gomperts, R. E. Stratmann, O. Yazyev, A. J. Austin, R. Cammi, C. Pomelli, J. W. Ochterski, R. L. Martin, K. Morokuma, V. G. Zakrzewski, G. A. Voth, P. Salvador, J. J. Dannenberg, S. Dapprich, A. D. Daniels, O. Farkas, J. B. Foresman, J. V. Ortiz, J. Cioslowski and D. J. Fox, *Gaussian 09, Revision D.01*, Gaussian, Inc., Wallingford CT, 2013.

